

Design of a Digital Adaptive Flight Control Law for the ALFLEX

Hideya Ito*, Yuzo Shimada** and Kenji Uchiyama***

*Graduate Student, **Professor, ***Assistant Professor

Department of Aerospace Engineering, College of Science and Technology, Nihon University
 7-24-1 Narashinodai, Funabashi, Chiba 274-8501, Japan
 (Phone: +81-47-469-5390; Fax: +81-47-467-9569; E-mail: shimada@aero.cst.nihon-u.ac.jp)

Abstract: In this report, a longitudinal adaptive flight control law is presented for the automatic landing system of a Japanese automatic landing flight experiment vehicle (ALFLEX). The longitudinal adaptive flight control law is designed to track an output of the vehicle to a guidance signal from the guidance portion of the automatic landing system. The proposed adaptive control law in the attitude control portion adjusts the controller gains continuously online as flight conditions change, in spite of the existence of unmodeled dynamics. The number of the controller gains to be adjusted is decreased to 1/2 from the previous studies. Computer simulation involving six-degree-of-freedom (DOF) nonlinear flight dynamics is performed to examine the effectiveness of the proposed adaptive control law. In order to verify the influence of the dispersion of the initial conditions, the Monte Carlo simulation is also applied. The initial conditions are more widely dispersed than the previous studies. As a result, except under the unsuitable initial conditions, the ALFLEX successfully landed on the runway.

Keywords: Adaptive Control, Aerospace Vehicle, Automatic Landing, ALFLEX

1. INTRODUCTION

In the development of a future space plane, automatic landing is a key technique that should be established. Since the space plane is expected to fly in an extremely wide flight envelope compared with those of conventional vehicles, the flight control system is required to deal with greater changes in the dynamics.

A Japanese automatic landing flight experiment vehicle (ALFLEX) was developed in order to examine and establish automatic landing techniques for the space plane. However, many of the studies on the flight control system for the ALFLEX have focused on the design of the optimal tuning of the system parameters or a gain-scheduled controller, while few studies have attempted to employ recent adaptive control theory [1-3]. This seems to be because of the ideal conditions imposed on the adaptive theory.

As reported in Refs. 4-6, we designed an adaptive control law for the ALFLEX longitudinal flight control system, where the vehicle's dynamics are treated as a discrete time linear-parameter-varying (LPV) system. In the designs, the vehicle's dynamics were assumed to be dependent on observable LPV parameters such as the dynamic pressure [7]. Furthermore, the influence of unmodeled dynamics was treated by imitating a part of the result reported in Ref. 8. However, it was revealed that the convergence of the estimated parameters was not sufficient due to the number of excess parameters to be estimated.

Therefore, in this study, we attempt to decrease the number of parameters to be estimated in the adaptive law in order to be able to treat the ALFLEX as a conventional linear-time-invariant (LTI) system with unknown constant parameters from the stand point that the ALFLEX flight envelope is limited to a part of the whole flight envelope for the space planes. Namely, the ALFLEX control system is designed to

estimate unknown constant parameters in the vehicle's dynamics.

Furthermore, although in the previous ALFLEX simulations, the program, provided by the National Aerospace Laboratory of Japan (NAL), was written in FORTRAN [9], in this study, we attempted to construct the ALFLEX simulation program in the MATLAB/Simulink environment.

Finally, in order to verify the effectiveness of the proposed adaptive flight control law, numerical simulation was performed. Also, the effects of the initial condition dispersion were examined with the Monte Carlo simulation method under a wider initial dispersion than that in the previous studies [4-6].

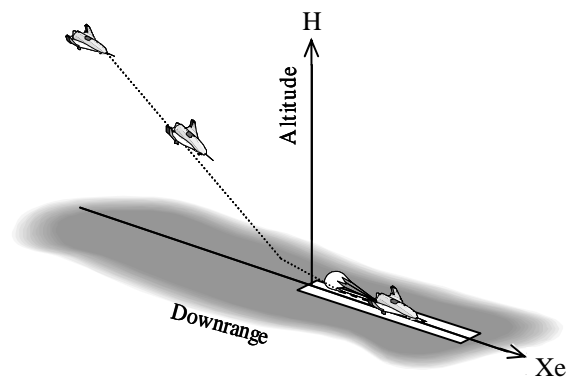


Fig.1 Automatic Landing Flight Experiment.

2. VEHICLE EQUATIONS OF MOTION

In the design of a longitudinal control system, if we choose z-directional acceleration as a controlled variable, the system becomes a nonminimum phase system. To avoid this difficulty, as the controlled variable $y(t)$, we choose a weighted linear

combination of the pitch rate q (rad/s), the acceleration a_z (m/s^2) at the center of gravity (C.G.) of the vehicle, and the angular acceleration \dot{q} (rad/s^2) as

$$y(t) = V_{co} \cdot q(t) - a_{zj}(t), \quad (1a)$$

$$a_{zj}(t) = a_z(t) - l \cdot \dot{q}(t), \quad (1b)$$

where V_{co} is a weight (which is usually called a crossover speed although, it does not have this meaning here), a_{zj} (m/s^2) is the acceleration at a point where the accelerometer is placed, and l is the distance between the accelerometer and the vehicle's C.G.

A command signal u_c to the control system is modified similarly to Eqs. (1a) and (1b) as

$$u_c(t) = V_{co} \cdot q_c(t) - a_{zjc}(t), \quad (2a)$$

$$a_{zjc}(t) = a_{zc}(t) - l \cdot \dot{q}_c(t). \quad (2b)$$

The continuous time equations representing the short-period motion can be expressed in state space form as

$$\dot{\mathbf{x}}(t) = \mathbf{A}_c \mathbf{x}(t) + \mathbf{b}_c u(t), \quad (3a)$$

$$y(t) = \mathbf{c}^T \mathbf{x}(t) = -a_z(t) + l \cdot \dot{q}(t) + V_{co} \cdot q(t). \quad (3b)$$

Here, the state vector and control input are defined as

$$\mathbf{x}(t) = [w(t), q(t), \delta_e(t)]^T, \quad (3c)$$

$$u(t) = \delta_{ec}(t), \quad (3d)$$

and the associate matrices are

$$\mathbf{A}_c = \begin{bmatrix} Z_w & U_0 & Z_{\delta_e} \\ M_w Z_w + M_w & M_w U_0 + M_q & M_w Z_{\delta_e} + M_{\delta_e} \\ 0 & 0 & -\omega_B \end{bmatrix}, \quad (3e)$$

$$\mathbf{b}_c = \begin{bmatrix} 0 \\ 0 \\ \omega_B \end{bmatrix}, \quad \mathbf{c} = \begin{bmatrix} l(M_w Z_w + M_w) - Z_w \\ l(M_w U_0 + M_q) + V_{co} \\ l(M_w Z_{\delta_e} + M_{\delta_e}) - Z_{\delta_e} \end{bmatrix}. \quad (3f, g)$$

Here, w is the z-directional velocity, δ_e (rad) the elevator deflection, and δ_{ec} (rad) the elevator deflection command which is equal to the control input u (rad) to the controlled system. Also, U_0 is the vehicle velocity, ω_B the actuator's bandwidth, and $Z_w, Z_{\delta_e}, M_w, M_q, \dots$ the dimensional stability derivatives, which are assumed to be constant unlike those in the previous studies.

3. DISCRETE MODEL OF THE PLANT WITH UNMODELED DYNAMICS

By adding a zero-order hold to the input of system (3), then taking the z-transform of the equations with respect to the sampling period T , the discrete time state equation and output equation can be expressed by

$$\mathbf{x}(k+1) = \mathbf{A}_p \mathbf{x}(k) + \mathbf{b}_p u(k), \quad (4a)$$

$$y(k) = \mathbf{c}^T \mathbf{x}(k), \quad (4b)$$

$$\mathbf{A}_p = e^{\mathbf{A}_c T}, \quad \mathbf{b}_p = \int_0^T e^{\mathbf{A}_c \tau} d\tau \cdot \mathbf{b}_c. \quad (4c)$$

Equation (4) can be transformed into the impulse transfer function as

$$y(k) = \frac{z^{-1} B(z^{-1})}{A(z^{-1})} \{1 + \Delta(z^{-1})\} u(k), \quad (5a)$$

$$A(z^{-1}) = 1 + a_1 z^{-1} + a_2 z^{-2} + a_3 z^{-3}, \quad (5b)$$

$$B(z^{-1}) = b_0 + b_1 z^{-1} + b_2 z^{-2}. \quad (5c)$$

Here, $z^{-1} B(z^{-1})/A(z^{-1})$ expresses the transfer function of a nominal portion of the controlled system (plant) expressed by Eq. (4), and $\Delta(z^{-1})$ expresses an unmodeled portion neglected in modeling the plant. Furthermore, $A(z^{-1})$, $B(z^{-1})$, and $\Delta(z^{-1})$ are assumed to be stable. In addition to them, note that z is used as a z-transform operator and z^{-1} is also used as a delay operator throughout this study.

At this point, Eq. (5a) can be rewritten as

$$A(z^{-1})y(k+1) = B(z^{-1})u(k) + v(k), \quad (6a)$$

$$v(k) = \Delta(z^{-1})B(z^{-1})u(k). \quad (6b)$$

Here, $v(k)$ is regarded as a disturbance signal due to the modeling error.

4. DESIGN OF AN ADAPTIVE CONTROL LAW

The aim of our study is to generate an adaptive control input $u(k)$ such that the vehicle's (plant's) output y can follow a guidance command u_c in spite of a modeling error in the vehicle's linearized dynamics.

Next, it is known that the polynomials $R(z^{-1})$ and $H(z^{-1})$ which satisfy the following relationship are uniquely determined.

$$D(z^{-1}) = A(z^{-1})R(z^{-1}) + z^{-d}H(z^{-1}), \quad (7a)$$

$$A(z^{-1}) = 1 + a_1 z^{-1} + a_2 z^{-2} + \dots + a_n z^{-n}, \quad (7b)$$

$$D(z^{-1}) = 1 + d_1 z^{-1} + d_2 z^{-2} + \dots + d_q z^{-q}, \quad (7c)$$

$$R(z^{-1}) = 1 + r_1 z^{-1} + r_2 z^{-2} + \dots + r_{d-1} z^{-(d-1)}, \quad (7d)$$

$$H(z^{-1}) = h_0 + h_1 z^{-1} + h_2 z^{-2} + \dots + h_p z^{-p}. \quad (7e)$$

In this study, we set them as

$$D(z^{-1}) = 1 + d_1 z^{-1} + d_2 z^{-2} + d_3 z^{-3}, \quad (8a)$$

$$R(z^{-1}) = 1, \quad (8b)$$

$$H(z^{-1}) = h_0 + h_1 z^{-1} + h_2 z^{-2}. \quad (8c)$$

By multiplying $y(k+1)$ on both sides of Eq. (7a) and substituting Eq. (6) into the result, Eq. (7a) can be rewritten as

$$\begin{aligned} D(z^{-1})y(k+1) &= B(z^{-1})u(k) + H(z^{-1})y(k) + v(k) \\ &= \hat{\theta}^T \xi(k) + \Delta(z^{-1})B(z^{-1})u(k) \end{aligned} \quad (9a)$$

where

$$\theta = [b_0, b_1, b_2, h_0, h_1, h_2]^T = [b_0, \hat{\theta}]^T = [\theta, \hat{\theta}]^T, \quad (9b)$$

$$\begin{aligned} \xi(k) &= [u(k), u(k-1), u(k-2), y(k), y(k-1), y(k-2)]^T \\ &= [u(k), \bar{\xi}(k)]^T \end{aligned} \quad (9c)$$

At this point, let us assume that an adaptive control input $u(k)$ that tracks the vehicle's output $y(k)$ to the command signal $u_c(k)$ generated in the guidance block is obtained by

$$u(k) = \frac{D(z^{-1})u_c(k+1) - \hat{\theta}^T(k)\bar{\xi}(k) - f(k)}{\hat{\theta}_1(k)}, \quad (10a)$$

$$\hat{\theta}(k) = [\hat{\theta}_1(k), \hat{\theta}(k)]^T, \quad (10b)$$

$$\xi(k) = [u(k), \bar{\xi}(k)]^T. \quad (10c)$$

Here, $\hat{\theta}(k)$ is a parameter estimation vector (variable gain) and $f(k)$ is an auxiliary signal generated by a feedback compensator which is employed to improve the loss of control performance caused by the second disturbance term in Eq. (9a). According to Ref. 8, $f(k)$ is generated using an observed output tracking error,

$$f(k) = D(z^{-1})P(z^{-1})e(k), \quad (11)$$

where the tracking error signal is defined as

$$e(k) = y(k) - u_c(k). \quad (12)$$

From Eq. (10a),

$$D(z^{-1})u_c(k+1) = \hat{\theta}^T(k)\xi(k) + f(k). \quad (13)$$

The error equation is obtained using Eqs. (9a), (12), and (13)

$$\begin{aligned} D(z^{-1})e(k+1) &= \psi^T(k)\xi(k) + \Delta(z^{-1})B(z^{-1})u(k) \\ &\quad - D(z^{-1})P(z^{-1})e(k+1) \end{aligned} \quad (14)$$

where $\psi(k)$ is a parameter estimation error and is defined as

$$\psi(k) = \theta - \hat{\theta}(k). \quad (15)$$

Eq. (14) can be rewritten as

$$\{1 + P(z^{-1})\}D(z^{-1})e(k+1) = \psi^T(k)\xi(k) + \Delta(z^{-1})B(z^{-1})u(k). \quad (16)$$

The compensator is determined in order to stabilize the following polynomial

$$1 + P(z^{-1}) = 1 + p_1 z^{-1}. \quad (17)$$

Thus, the adaptive control input is determined by

$$u(k) = \frac{D(z^{-1})u_c(k+1) - \hat{\theta}^T(k)\bar{\xi}(k) - D(z^{-1})p_1 e(k)}{\hat{\theta}_1(k)}. \quad (18)$$

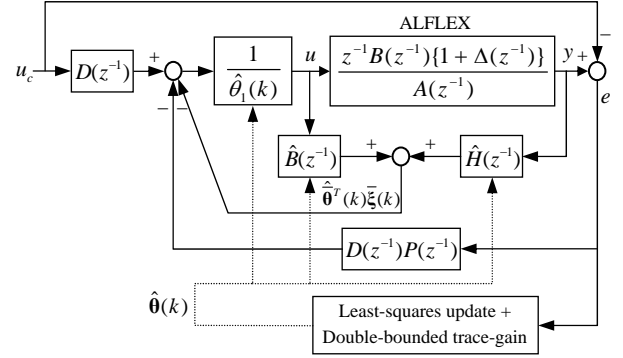


Fig.2 Block diagram for the adaptive flight control system.

5. PARAMETER ADJUSTMENT LAW

The parameter $\hat{\theta}(k)$ is estimated by the least-squares update formula,

$$\hat{\theta}(k) = \hat{\theta}(k-1) - \frac{\Pi(k-1)\xi(k-1)\{\hat{\theta}^T(k-1)\xi(k-1) - D(z^{-1})y(k)\}}{1 + \xi^T(k-1)\Pi(k-1)\xi(k-1)}, \quad (19a)$$

$$\begin{aligned} \Pi(k) &= \frac{1}{\lambda(k)} \left[\Pi(k-1) - \frac{\Pi(k-1)\xi(k-1)\xi^T(k-1)\Pi(k-1)}{1 + \xi^T(k-1)\Pi(k-1)\xi(k-1)} \right] \\ &= \frac{1}{\lambda(k)} \Pi'(k) \end{aligned} \quad (19b)$$

Where, $\lambda(k)$ is a forgetting factor and is obtained using a double-bounded trace-gain algorithm [10],

$$\lambda(k) = \begin{cases} \text{tr}\Pi'(k)/\gamma_u ; \lambda \leq \text{tr}\Pi'(k)/\gamma_u \\ \lambda ; \text{tr}\Pi'(k)/\gamma_u \leq \lambda \leq \text{tr}\Pi'(k)/\gamma_l \\ \text{tr}\Pi'(k)/\gamma_l ; \text{tr}\Pi'(k)/\gamma_l \leq \lambda \end{cases} \quad (20a)$$

$$\Pi(0) = \Pi^T(0) > 0, \quad 0 < \gamma_l < \text{tr}\Pi(0) \leq \gamma_u, \quad 0 < \lambda < 1. \quad (20b)$$

6. NUMERICAL SIMULATIONS

In order to examine the effectiveness of the proposed design, numerical simulation was performed in the MATLAB/Simulink environment. In the simulation, the stable polynomials in Eqs. (8a) and (17) were selected as follows:

$$D(z^{-1}) = 1 - 0.2375z^{-1} + 0.0206z^{-2} + 0.0489z^{-3}, \quad (21)$$

$$1 + P(z^{-1}) = 1 + 0.7788z^{-1}. \quad (22)$$

First, a flight simulation with nominal initial conditions [9] was carried out. The ALFLEX is released at a level speed of 46.0(m/s), a height of 1500(m), and a downrange of -2782(m).

Figures 3-4 show the behaviors of the controller gains (parameter estimation) adjusted by the adaptive algorithm. The gains manage to follow their true values on the whole. Figure 5 shows the time responses of the output $y(t)$ and the command signal $u_c(t)$ generated in the basic guidance system provided. A glance at Fig.5 reveals that the ALFLEX output coincides well with the command signal. Figure 6 shows the time responses of the elevator deflection command $\delta_{ec}(t)$ and elevator deflection $\delta_e(t)$. The magnitude of the control is within the allowable range of +25(deg) and -35(deg) except that the vehicle is on the runway. Figure 7 shows the flight path and the reference flight path. The ALFLEX follows its reference flight path well from approximately 2000(m) ahead of the runway and successfully touches down on the runway. Figure 8 shows the vehicle velocity and the reference velocity. The vehicle velocity tracks its reference velocity well.

Finally, the influences of the initial condition dispersion are examined using the Monte Carlo method [1, 2]. In Refs.4-6, the initial condition was dispersed while satisfying a trim condition. However, the actual flight path is considered to be part of the trajectory of a space plane. Therefore, the trim condition of the horizontal flight in the initial state was relaxed in this study. Table 1 shows the initial conditions and the values of each 3σ used in the simulation.

Table 1 Initial condition and each 3σ .

| | Nominal | 3σ |
|-------------------|---------|-----------|
| Downrange | -2782 m | 300 m |
| Altitude | 1500 m | 300 m |
| Velocity | 46 m/s | 30 m/s |
| Flight path angle | -30 deg | 15 deg |
| Angle of attack | 7 deg | 15 deg |

Figures 9-11 show the dispersed initial positions, the initial velocities, and the initial angles, respectively. Figures 12 and 13 show the dispersion of the vertical and horizontal trajectory profiles after 100 repetitions of the Monte Carlo simulation. Figure 14 shows the dispersion of the velocity profiles of the Monte Carlo simulation.

Figure 15 shows the result of the percentage of success after 100 repetitions of the Monte Carlo simulation. The results indicate that in 93% of the examined cases, the ALFLEX could successfully touch down on the runway. Also, note that the common feature in the unsuccessful cases tends to be the initial condition of a low speed which results in an unacceptably large magnitude of acceleration command for a limiter in the guidance block.

Figure 16 shows the touchdown positions after 100 repetitions of the Monte Carlo simulation.

7. SUMMARY

In this study, we presented an adaptive control law for an ALFLEX model, which has unknown but constant parameters, for tracking a guidance signal. The obtained controller allows estimation error and a certain kind of modeling error. In the numerical simulations of an automatic landing, we applied the present method for the control of the longitudinal motion of the ALFLEX. The 6-DOF-simulation results revealed that the ALFLEX output follows the reference command very well, the adjusted parameters estimate their true values quite well, and the ALFLEX successfully touched down while satisfying landing conditions with a percentage of success of 93% against initial condition dispersion.

REFERENCES

- [1] Y. Miyazawa and T. Motoda, "Stochastic Parameter Turning Applied to Space Vehicle Flight Control Design," *Journal of Guidance, Control, and Dynamics*, Vol.24, No.3, pp.597-604, May-June 2001.
- [2] Y. Minami, Y. Miyazawa, and Y. Shimada, "Stochastic Design Approach for the Guidance and Control System of an Automatic Landing Vehicle," *Proceedings of the 13th Korea Automatic Control Conference*, Pusan, Korea, pp.41-46, 1998.
- [3] A. Ohara, M. Ide, Y. Yamaguchi, and M. Ohno, "LPV Modeling and Gain Scheduled Control of ALFLEX Vehicle Flight Systems," *ISCIE*, Vol.12, No.11, pp.655-663, 1999.
- [4] K. Imai, "Design of An Adaptive Flight Control Law for the ALFLEX Using an LPV Model (in Japanese)," *Master's Thesis at the Graduate School of Science and Technology, Nihon University*, March 2002.
- [5] Y. Shimada and K. Uchiyama, "An Automatic Landing System Using Adaptive Control for a Re-entry Vehicle," *ISTS 2002-d-60, 23rd International Symposium on Space Technology and Science*, Matsue, Shimane, Japan, May 2002.
- [6] Y. Shimada and K. Uchiyama, "Redesign of the Adaptive Flight Control Law for the ALFLEX Flight Control System," *2002 International Conference on Control, Automation, and Systems*, Muju Resort, Korea, pp.239-244, October 16-19, 2002.
- [7] Y. Shimada, N. Kobayashi, and H. Miyazawa, "A Digital Adaptive Flight Control System Design for Aircraft with Varying Stability Derivatives," *Journal of the Japan Society for Aeronautical and Space Sciences*, Vol. 36, No. 413, pp. 304-311, 1988.
- [8] K. Itamiya, Y. Suzuki, and T. Suzuki, "A Robust Scheme for the Direct MRACS and Its Stability Analysis," *SICE*, Vol.34, No.10, pp.1425-1433, 1998.
- [9] NAL/NASDA ALFLEX Group, "Flight Simulation Model for Automatic Landing Flight Experiment," *Technical Report of National Aerospace Laboratory, NAL TR-1252*, 1994.
- [10] S. Shinnaka and T. Suzuki, "New Parameter Adjustment Algorithms for Adaptive Systems," *SICE*, Vol.21, No.7, pp.691-697, 1985.

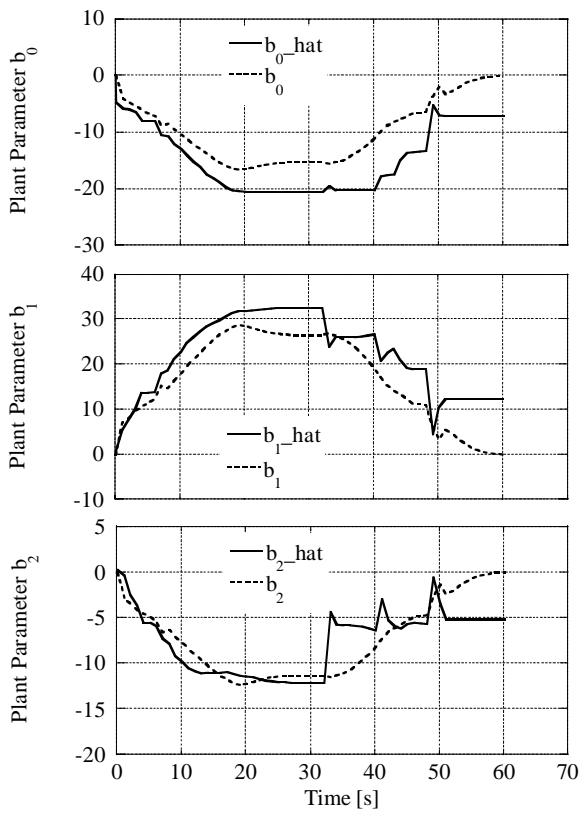


Fig.3 Estimation of the numerator.

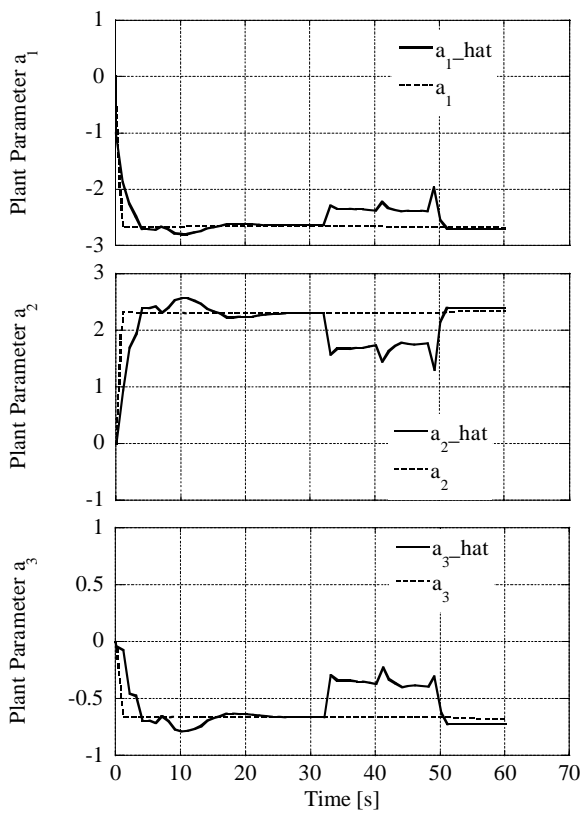


Fig.4 Estimation of the denominator.

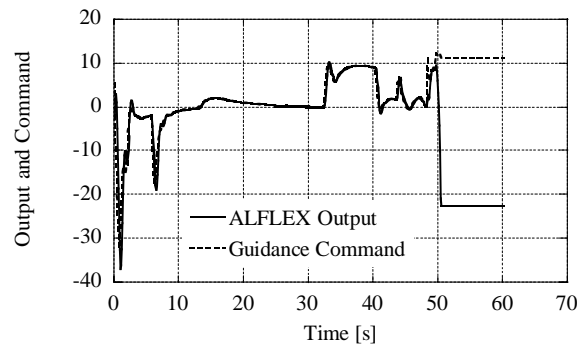


Fig.5 Comparison of output with command signal.

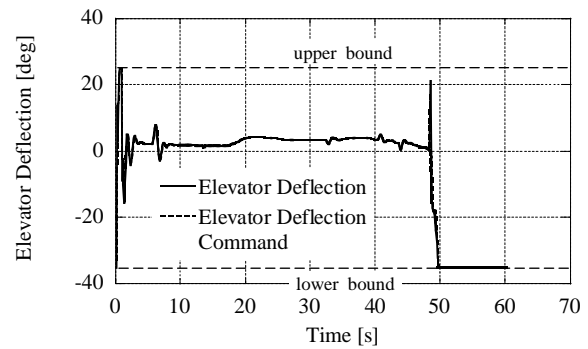


Fig.6 Elevator deflection and its command.

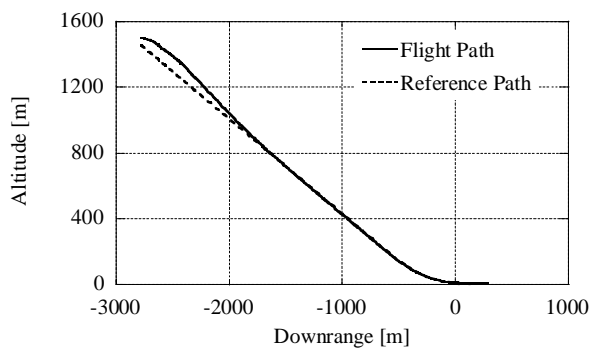


Fig.7 Flight path and reference path.

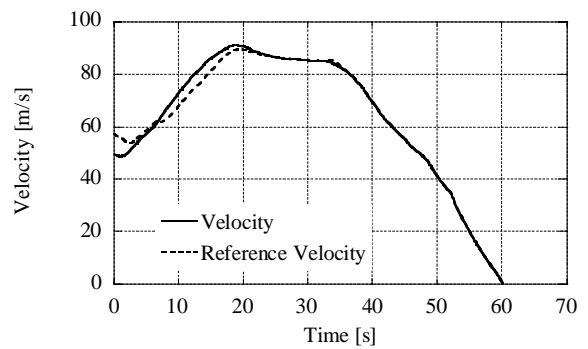


Fig.8 Velocity and reference velocity.

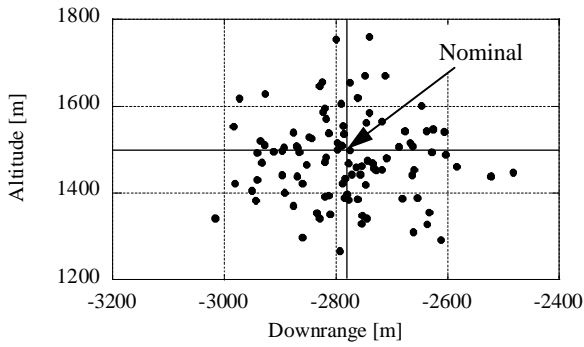


Fig.9 Initial position dispersion.

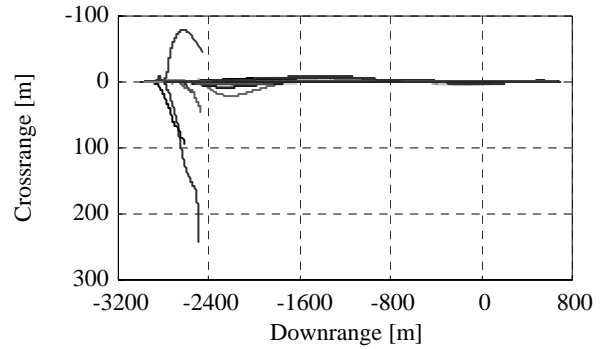


Fig.13 Horizontal trajectory profiles due to initial condition dispersion.

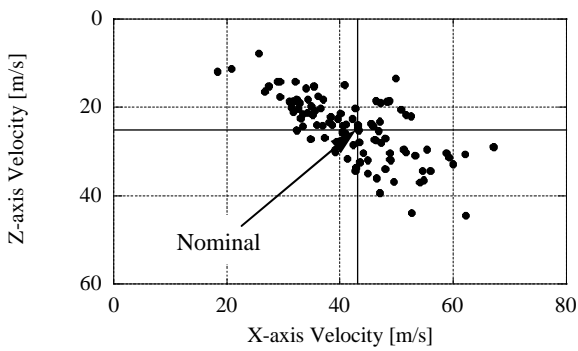


Fig.10 Initial velocity dispersion.

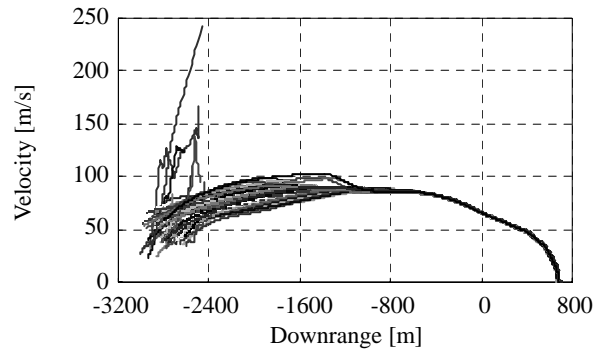


Fig.14 Velocity profiles due to initial condition dispersion.

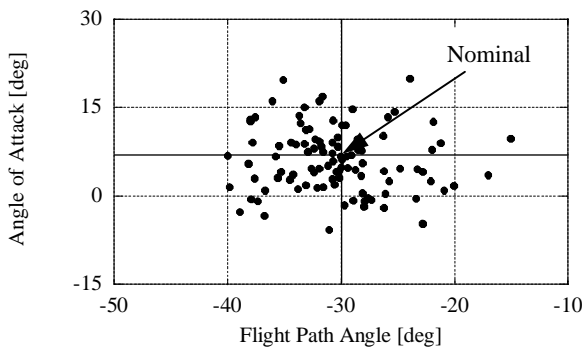


Fig.11 Initial angle dispersion.

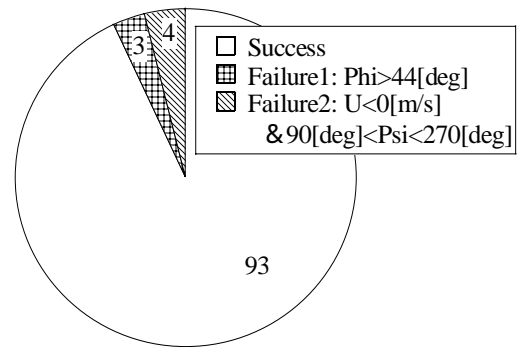


Fig.15 Result after 100 repetitions of the Monte Carlo simulation.

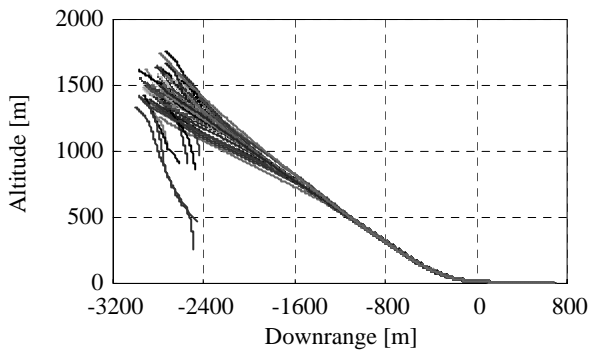


Fig.12 Vertical trajectory profiles due to initial condition dispersion.

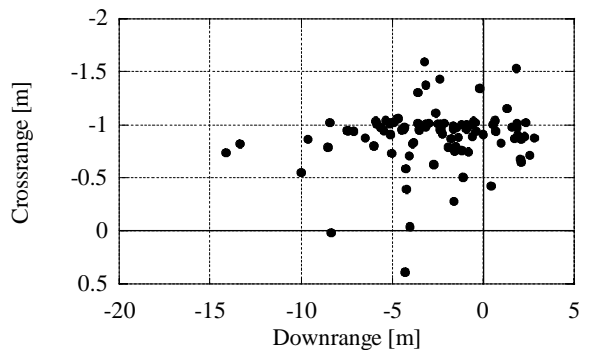


Fig.16 Touchdown positions.